On the implementation of symmetric and antisymmetric periodic boundary conditions for incompressible flow

Report 93-61

Guus Segal
Kees Vuik
Kees Kassels

TU Delft
Faculteit der Technische Wiskunde en Informatica
Faculty of Technical Mathematics and Informatics

Technische Universiteit Delft
Delft University of Technology

ISSN 0922-5641

Copies of these reports may be obtained from the bureau of the Faculty of Technical Mathematics and Informatics, Julianalaan 132, 2628 BL Delft, phone +3115784568.
A selection of these reports is available in PostScript form at the Faculty's anonymous ftp-site. They are located in the directory /pub/publications/tech-reports at ftp.twi.tudelft.nl

On the implementation of symmetric and antisymmetric periodic boundary conditions for incompressible flow

Guus Segal
Kees Vuik
Kees Kassels

Abstract

In this paper we consider symmetric and antisymmetric periodic boundary conditions for flows governed by the incompressible Navier-Stokes equations. Classical periodic boundary conditions are studied as well as symmetric and antisymmetric periodic boundary conditions in which there is a pressure difference between inlet and outlet. The implementation of this type of boundary conditions in a finite element code using the penalty function formulation is treated and also the implementation in a finite volume code based on pressure correction. The methods are demonstrated by computation of a flow through a staggered tube bundle.

1 Introduction

In many papers and text books ([1] - [8]) discretizations of the incompressible Navier-Stokes equations are described. However, in general not much attention is paid to the incorporation of boundary conditions. But for engineering applications the implementation of adequate boundary conditions is equally important for accuracy as the formulation and discretization of the differential equations itself. In this paper we shall consider three types of periodic and anti-periodic boundary conditions, namely

- periodicity in velocity and pressure
- periodicity in velocity and periodicity in pressure gradient
- antisymmetric periodicity in velocity and pressure gradient

The last two boundary conditions are combined with prescription of a given flow rate.

Pure periodic boundary conditions arise for example in the case of an artificial cut in a region. Such artificial cuts naturally arise in the computation of a flow around an obstacle by finite volume techniques.

Periodicity in velocity and pressure gradient in combination with a prescribed flow rate naturally arises in the case of a periodically repeated configuration.

For example, experiments in a bundle of 7 horizontal staggered pipes (Figure 1) by Simonin and Barcouda (1988) [7], show that for water flowing upwards at an average velocity of 1.06 m/s the flow becomes periodic around the fourth row from the bottom. Hence for the flow in the interior it suffices to compute the flow in the dashed computational region only. In this example the boundaries Γ_2, Γ_4 and Γ_5 are symmetry boundaries, whereas Γ_1 and Γ_3 are periodic boundaries. In order to have a flow it is necessary that the pressures at left-hand side and right-hand side differ a constant. This unknown constant may be given implicitly by prescribing the flow rate Q.

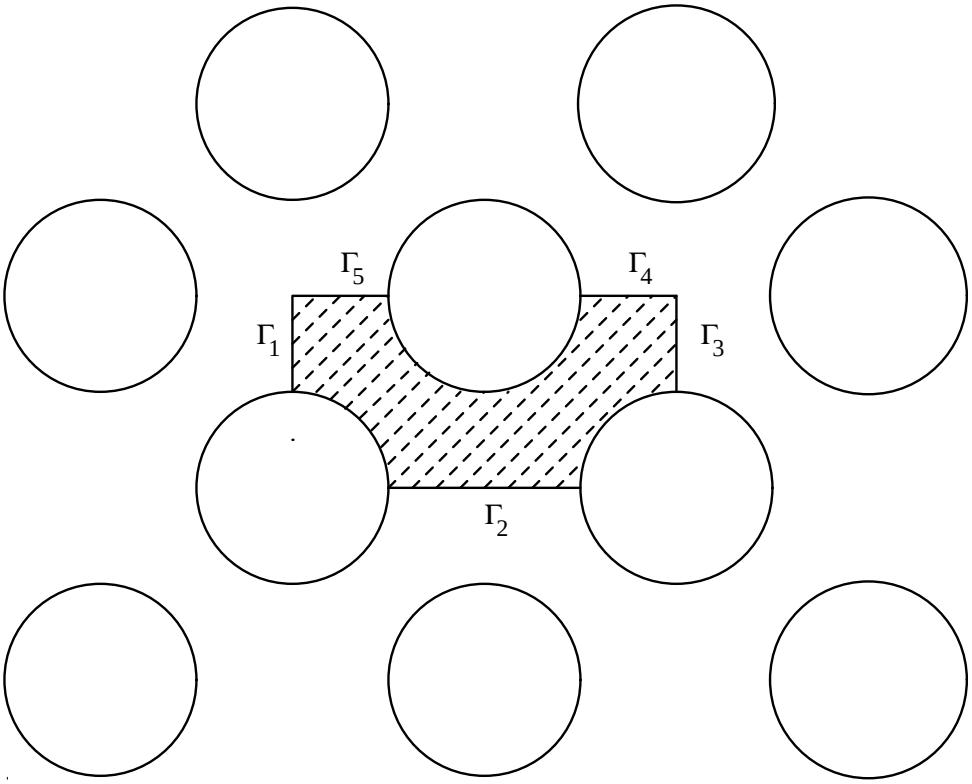

Figure 1: Computational region in array of staggered pipes with periodic boundary conditions.

In this particular problem it is possible to reduce the computational domain still further by halving, as shown in Figure 2. In that case the boundary conditions at the boundaries Γ_1 and Γ_3 are antisymmetric periodic instead of symmetric.

Periodic boundary conditions with a given flow rate in combination with finite element methods have been treated by Fortin [2]. He uses an Uzawa-type scheme to solve the incompressible Navier-Stokes equations. We shall extend his ideas to antiperiodic boundary conditions in combination with a penalty function formulation.
Perić [5] treats anti-symmetric periodic boundary conditions in combination with a finite volume method. He uses artificial cells at the inlet and outlet which are copies of the cells at the other side. Starting with some initial field, the flow at the next time-step is computed. As

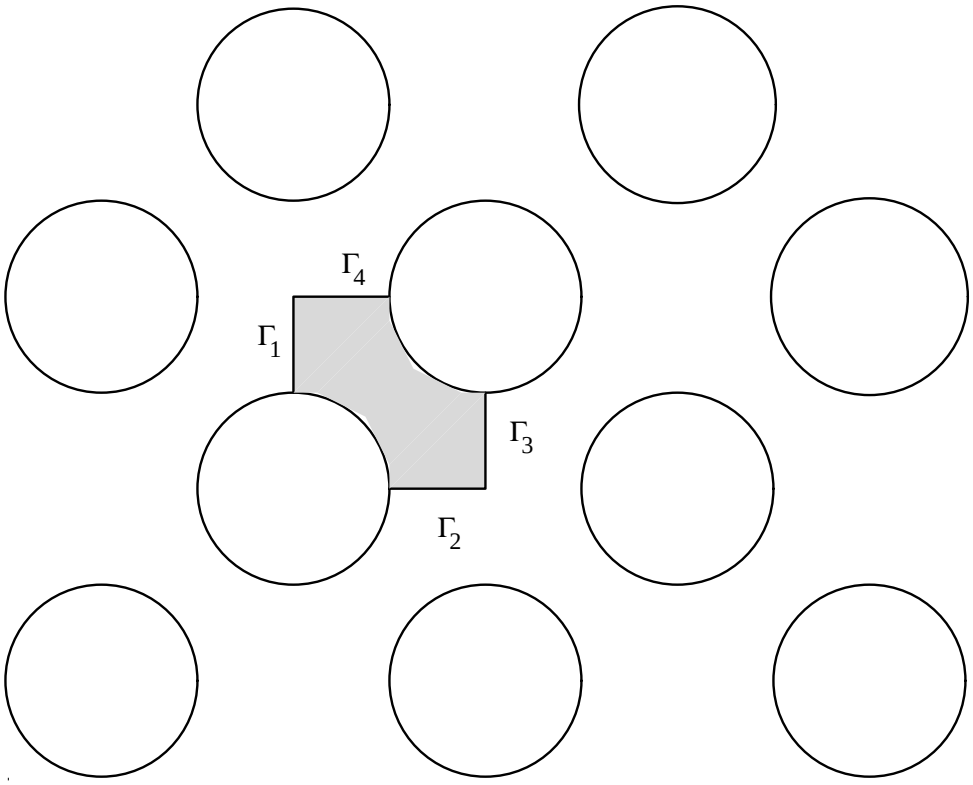

Figure 2: Computational region in array of staggered pipes with anti-periodic boundary conditions.

boundary conditions at inlet and outlet the computed velocities at the corresponding other sides are copied from the preceding iteration. By iterating this process converges to the correct values. However, this process requires approximately 2 to 3 times the usual number of iterations.

2 Formulation of the problem

We consider the instationary incompressible Navier-Stokes equations in general co-ordinates

$$\frac{\partial}{\partial t}(\rho U^\alpha) + (\rho U^\alpha U^\beta)_{,\beta} + (g^{\alpha\beta} p)_{,\beta} - \tau^{\alpha\beta}_{,\beta} = \rho f^\alpha \tag{1}$$

$$U^\alpha_{,\alpha} = 0 \tag{2}$$

where $\tau^{\alpha\beta}$ represents the deviatoric stress tensor

$$\tau^{\alpha\beta} = \mu(g^{\alpha\gamma} U^\beta_{,\gamma} + g^{\gamma\beta} U^\alpha_{,\gamma}), \tag{3}$$

with μ the viscosity, p the pressure, U^α the contravariant velocity component and ρ the density of the fluid. In this formulation the standard tensor notation with summation convention is

used. $g^{\alpha\beta}$ represents the metric tensor. See Segal et al [6], Oosterlee and Wesseling [4], Wesseling et al [11], and Mynett et al [3] for the details. In our present study we restrict ourselves to laminar, stationary flow although the work is motivated by a turbulent problem.

For the sake of argument we restrict ourselves to a rectangular domain as shown in Figure 3 with periodicity at the inlet and outlet boundaries Γ_1 and Γ_3. We consider the following types of periodicity:

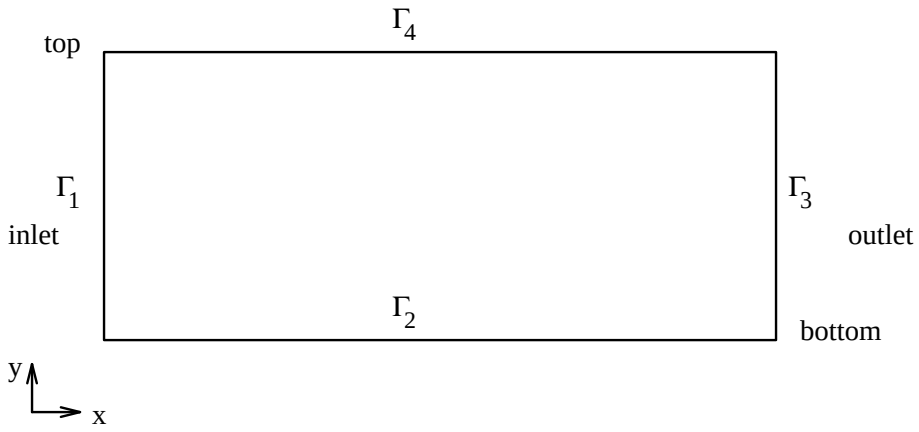

Figure 3: Periodicity at a rectangular domain.

- pure periodicity

  In this case the boundary conditions are given by

$$\begin{aligned} \boldsymbol{u}_{left} &= \boldsymbol{u}_{right}\ ,\ p_{left} = p_{right}, \\ \frac{\partial \boldsymbol{u}}{\partial n}|_{left} &= -\frac{\partial \boldsymbol{u}}{\partial n}|_{right}, \end{aligned} \tag{4}$$

  which $\boldsymbol{u}$ the velocity vector, and n the outward directed normal. The subscript left and right indicate that the values at the left respectively right-hand side are meant. Of course $\boldsymbol{u}$ and p may vary along these boundaries.

- periodicity with unknown jump in pressure

  The boundary conditions for the velocity are the same as in (4) however there is a constant pressure difference between left-hand side and right-hand side.
  So

$$\boldsymbol{u}_{left} = \boldsymbol{u}_{right}\ , \tag{5a}$$

$$\frac{\partial \boldsymbol{u}}{\partial n}|_{left} = -\frac{\partial \boldsymbol{u}}{\partial n}|_{right}\ , \tag{5b}$$

$$p_{left} = p_{right} + c \tag{5c}$$

To fix the unknown constant c an extra condition is necessary. It is quite natural to prescribe the flow rate Q:

$$Q = -\int_{\Gamma_1} \boldsymbol{u} \cdot \boldsymbol{n} d\Gamma \tag{6}$$

- anti-symmetric periodicity with unknown jump in pressure

This boundary condition very much resembles that of (5a - 5c), (6). However, the tangential velocity component and the tangential direction get opposite signs. Hence:

$$\begin{aligned}
\boldsymbol{u} \cdot \boldsymbol{n}(y)|_{left} &= \boldsymbol{u} \cdot \boldsymbol{n}(y_{top} - y)|_{right}, && (7a)\\
\boldsymbol{u} \cdot \boldsymbol{t}(y)|_{left} &= -\boldsymbol{u} \cdot \boldsymbol{t}(y_{top} - y)|_{right}, && (7b)\\
\frac{\partial \boldsymbol{u} \cdot \boldsymbol{n}}{\partial n}(y)|_{left} &= -\frac{\partial \boldsymbol{u} \cdot \boldsymbol{n}}{\partial n}(y_{top} - y)|_{right}, && (7c)\\
\frac{\partial \boldsymbol{u} \cdot \boldsymbol{t}}{\partial n}(y)|_{left} &= \frac{\partial \boldsymbol{u} \cdot \boldsymbol{t}}{\partial n}(y_{top} - y)|_{right}, && (7d)\\
p(y)|_{left} &= p(y_{top} - y)|_{right} + c, && (7e)
\end{aligned}$$

where $\boldsymbol{t}$ is the tangential vector, which is taken from bottom to top.
Furthermore, condition (6) holds.

3 Solution by finite element techniques

To solve the incompressible Navier-Stokes equations, the standard Galerkin approach (SGA) is applied in this section. We restrict ourselves to extended quadratic triangles of Crouzeix Raviart type (see Cuvelier et al [1]). Hence the velocity per element is approximated by an extended quadratic polynomial, and the pressure per element is a linear discontinuous polynomial.
With respect to the boundary conditions of section 2 we have to deal with two problems. One is the incorporation of periodic or anti-symmetric periodic boundary conditions. The other one is the incorporation of the given flow rate and corresponding unknown pressure constant c.

To implement the periodicity the unknowns at left-hand side and right-hand side are identified, which means that they refer to the same unknown. In the case of anti symmetric periodicity the sequence of the unknowns along the sides is reversed. Furthermore, the nodal points at left-hand side and right-hand side are coupled by so-called connection elements. These connection elements are nothing but dummy elements which indicate that with respect to the topology elements at the left-hand boundary are connected to elements at the right-hand boundary, although the co-ordinates are different.
If we denote the discretized velocities at the left-hand boundary by $\boldsymbol{u}_l$ and at the right-hand boundary by $\boldsymbol{u}_r$, the relations (5a) or (7a) and (7b) may be written as:

$$\boldsymbol{u}_l = D\boldsymbol{u}_r \ , \tag{8}$$

where D is a diagonal matrix containing diagonal elements 1 and -1 in the case of anti-symmetric boundary conditions and D is equal to the identity matrix in case of a symmetric periodic boundary condition. In fact our approach allows for general diagonal matrices D.
Now suppose that the system of equations to be solved is denote by

$$\boldsymbol{S}\boldsymbol{u} = \boldsymbol{f} \tag{9}$$

We split the vector $\boldsymbol{u}$ into three parts $\boldsymbol{u}_l$, $\boldsymbol{u}_r$ and u_i, where $\boldsymbol{u}_i$ denotes all unknowns not present at left-hand or right-hand boundary. The matrix S and the right-hand-side vector $\boldsymbol{f}$ are split correspondingly. Then system (9) can be written as:

$$\begin{bmatrix} \boldsymbol{S}_{ii} & \boldsymbol{S}_{il} & \boldsymbol{S}_{ir} \\ \boldsymbol{S}_{li} & \boldsymbol{S}_{ll} & \boldsymbol{S}_{lr} \\ \boldsymbol{S}_{ri} & \boldsymbol{S}_{rl} & \boldsymbol{S}_{rr} \end{bmatrix} \begin{bmatrix} \boldsymbol{u}_i \\ \boldsymbol{u}_l \\ \boldsymbol{u}_r \end{bmatrix} \begin{bmatrix} \boldsymbol{f}_i \\ \boldsymbol{f}_l \\ \boldsymbol{f}_r \end{bmatrix} \tag{10}$$

If we substitute relation (8) into (10), multiply the second equation by D and add the third equation to the second one, equation (10) reduces to:

$$S_{ii}u_i + (S_{il}D + S_{ir})u_r = f_i \tag{11a}$$

$$(DS_{li} + S_{ri})u_i + (DS_{ll}D + (S_{rl}D + DS_{lr}) + S_{rr})u_r = Df_l + f_r \tag{11b}$$

The multiplication is performed in order that the new matrix is still symmetric if the original matrix S is symmetric.

The implementation of (11a) and (11b) is straightforward in a finite element context. Before constructing the large matrix, it is sufficient to multiply the rows and columns corresponding to unknowns positioned at the left-hand boundary by the appropriate diagonal element. In the same way the element vector must be updated.
Finally in the post-processing stage relation (8) must be incorporated in order to get the overall velocity vector.

The implementation of the constraint (6) is done in penalty variant of the method described by Fortin [2].
Discretization of (6) gives a linear relation:

$$R\boldsymbol{u} = Q, \tag{12}$$

where R has non-zero contributions for all normal components of the velocity at the boundary. In case of a stationary Stokes equation the discretization of the equations (1) - (3) under the constraint (12) may be regarded as a minimization problem of the form:

$$\min_{\boldsymbol{u}} \frac{1}{2}\boldsymbol{u}^T\boldsymbol{S}\boldsymbol{u} - \boldsymbol{u}^T\boldsymbol{F}, \tag{13a}$$

under the constraints

$$\boldsymbol{L}\boldsymbol{u} = \boldsymbol{0}, \tag{13b}$$

$$\boldsymbol{R}\boldsymbol{u} = Q, \tag{13c}$$

Here $\boldsymbol{Su}$ represents the discretization of the stress tensor, $\boldsymbol{F}$ the discretization of the right-hand side and $\boldsymbol{Lu} = \boldsymbol{0}$ the discretization of the continuity equation.

One immediately shows that the Kuhn-Tucker relations associated with (13a-13c) can be formulated as:

$$\boldsymbol{Su} + \boldsymbol{L}^T\boldsymbol{p} + \boldsymbol{R}^T\lambda = \boldsymbol{F}, \tag{14a}$$

$$\begin{aligned} \boldsymbol{Lu} &= \boldsymbol{0}, & (14b)\\ \boldsymbol{Ru} &= Q. & (14c) \end{aligned}$$

In the case of a continuous pressure approximation with pressure unknowns at the boundary of the element (Taylor-Hood element), the parameter λ may easily be identified with the unknown constant c in (7e). In the case of a discontinuous pressure approximation, such an identification is no longer clear, although one may expect a strong relation between λ and c.

From (13a-13c) it is quit trivial that the penalty function formulation of the stationary Navier-Stokes equations under the constraint (12) becomes;

$$\boldsymbol{Su} + \boldsymbol{N}(\boldsymbol{u})\boldsymbol{u} + \sigma_1\boldsymbol{L}^T\boldsymbol{Lu} + \sigma_2\boldsymbol{R}^T\boldsymbol{Ru} = \boldsymbol{F} + \sigma_2\boldsymbol{R}^TQ, \tag{15}$$

where σ_1 and σ_2 are penalty parameters and $\boldsymbol{N}(\boldsymbol{u})\boldsymbol{u}$ denotes the discretization of the convection terms.

The matrix $\sigma_2\boldsymbol{R}^T\boldsymbol{R}$ and the right-hand-side term $\sigma_2\boldsymbol{R}^TQ$ are built using an element containing all normal components of the velocity at the inlet. The boundary conditions for the pressure are satisfied implicitly by formulation (15).

4 Solution by finite volume techniques

Our finite volume discretization of the incompressible Navier-Stokes equations is based on a boundary fitted staggered approach as described in [6], [4], [9], [3]. The curved grid is mapped onto a rectangular domain and the invariant formulation (1) - (3) of the Navier-Stokes equations is used. With respect to the mapping it is supposed that only co-ordinates of the vertices of the cells are known. All geometrical coefficients including Christoffel symbols are computed by finite differences of the co-ordinates. In order to decouple velocity and pressure computation a standard pressure correction method as described by van Kan [9] is used. The nonlinear equations are linearized by a standard Newton linearization and the systems of linear equations are solved by a preconditioned GMRESR method [10].

The position of the unknowns in the staggered grid in the computational domain is sketched in Figure 4.
In order to incorporate the periodic boundary condition (5a) or the anti-symmetric boundary condition (7a) the equations for the normal velocity components at the inlet boundary are replaced by trivial equations making velocity components at left-hand side and right-hand side identical:

$$\boldsymbol{u}\cdot\boldsymbol{n}|_{inlet} = \boldsymbol{u}\cdot\boldsymbol{n}|_{outlet}. \tag{16}$$

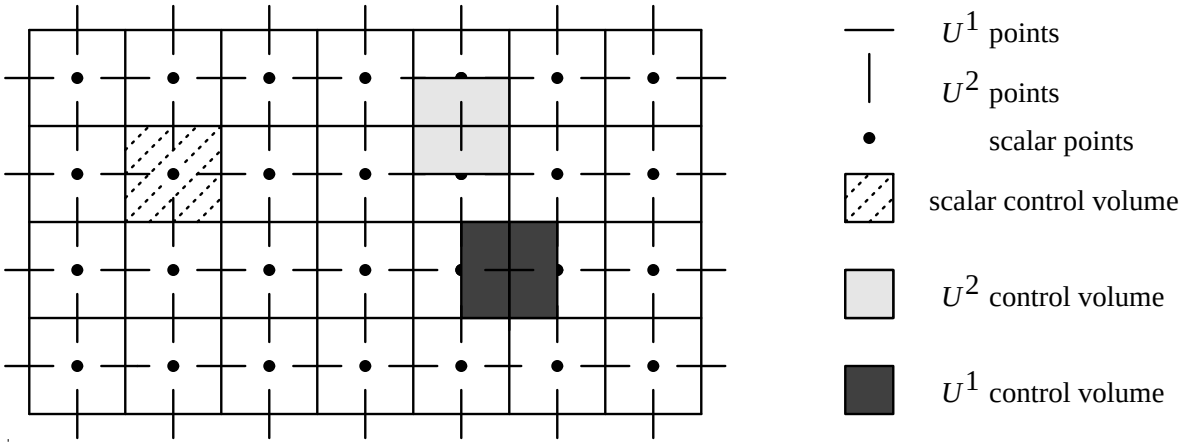

Figure 4: Position of unknowns in staggered grid

In the anti-symmetric case of course the correct unknowns must be coupled. In order to prescribe the other types of periodic boundary conditions, both at the left-hand side and right-hand side a column of virtual cells is introduced, see Figure 5.

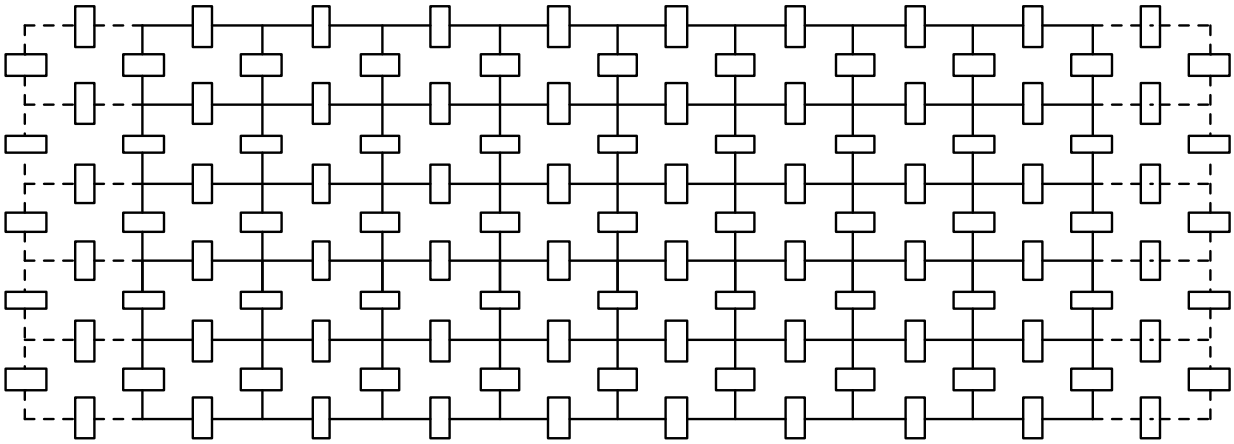

Figure 5: Extension of computational domain with virtual cells

The virtual unknowns in the virtual cells, however, are in fact the real unknowns at the other side taking the possible anti-symmetry into account. Of course in the virtual pressure unknowns it is necessary to incorporate the unknown pressure jump constant c from equation (5c). The standard finite volume method is applied for all internal velocity unknowns, but also for the normal components at the outlet boundary.

In this way we get the following system of instationary non-linear equations:

$$\boldsymbol{M}\boldsymbol{u} + \boldsymbol{S}\boldsymbol{u} + \boldsymbol{N}(\boldsymbol{u})\boldsymbol{u} + \boldsymbol{G}^T\boldsymbol{p} + \bar{\boldsymbol{G}}^T c = \boldsymbol{F}, \tag{17a}$$

$$\boldsymbol{D}\boldsymbol{u} = \boldsymbol{0}, \tag{17b}$$

$$\boldsymbol{R}\boldsymbol{u} \;=\; Q. \tag{17c}$$

$\boldsymbol{S}\boldsymbol{u}$, $\boldsymbol{N}(\boldsymbol{u})\boldsymbol{u}$, $\boldsymbol{R}\boldsymbol{u} = \boldsymbol{Q}$ and $\boldsymbol{F}$ have exactly the same meaning as in (14a-14c), although their contents are completely different. $\boldsymbol{G}^T\boldsymbol{p}$ represents the discretization of ∇p except for the unknown constant, whose contribution is stored in $\bar{\boldsymbol{G}}^T c$. Mark that the matrix $\bar{\boldsymbol{G}}$ has only non-zero entries in the points connected to inflow and outflow boundary. $\boldsymbol{D}\boldsymbol{u} = \boldsymbol{0}$ gives the discretization of the continuity equation and $\boldsymbol{M}\boldsymbol{u}$ the discretization of the time derivative. In fact $\boldsymbol{M}$ is a diagonal matrix containing the value of ρ multiplied by the area of the corresponding control volume as diagonal elements.

In order to solve equations (17a-17c) the standard Newton linearization is applied. Furthermore we extend the pressure correction method as described by van Kan [9] in order to incorporate the unknown c and the extra equation (17c).

If we apply a standard θ-method to (17a-17c), we get the following system of non-linear equations:

$$\begin{aligned} \boldsymbol{M}\frac{\boldsymbol{u}^{n+1}-\boldsymbol{u}^n}{\Delta t} \;&+\; \theta\tilde{\boldsymbol{S}}\boldsymbol{u}^{n+1} + (1-\theta)\tilde{\boldsymbol{S}}\boldsymbol{u}^n + \theta\boldsymbol{G}^T\boldsymbol{p}^{n+1} + (1-\theta)\boldsymbol{G}^T\boldsymbol{p}^n \\ &+\; \theta\bar{\boldsymbol{G}}^T c^{n+1} + (1-\theta)\bar{\boldsymbol{G}}^T c^n = \theta\tilde{\boldsymbol{F}}^{n+1} + (1-\theta)\tilde{\boldsymbol{F}}^n\,, \end{aligned} \tag{18a}$$

$$\boldsymbol{D}\boldsymbol{u}^{n+1} \;=\; \boldsymbol{0}, \tag{18b}$$

$$\boldsymbol{R}\boldsymbol{u}^{n+1} \;=\; 0. \tag{18c}$$

Here $\tilde{\boldsymbol{S}}$ denotes the contribution of $\boldsymbol{S}$ and the matrix part of the linearization of $\boldsymbol{N}(\boldsymbol{u})\boldsymbol{u}$. The right-hand side part of the linearization is put into the term $\tilde{\boldsymbol{F}}$.

Now we follow the usual approach with respect to pressure correction, where we treat the constant c in exactly the same way as the pressure $\boldsymbol{p}$. Hence in equation (18a) $\boldsymbol{u}^{n+1}$ is replaced by a predictor $\boldsymbol{u}^*$ and $\boldsymbol{p}$ and c are only introduced at the preceding time-level:

$$\boldsymbol{M}\frac{\boldsymbol{u}^*-\boldsymbol{u}^n}{\Delta t} + \theta\tilde{\boldsymbol{S}}\boldsymbol{u}^* + (1-\theta)\tilde{\boldsymbol{S}}\boldsymbol{u}^n + \boldsymbol{G}^T\boldsymbol{p}^n + \bar{\boldsymbol{G}}^T c^n = \tilde{\boldsymbol{F}}^{n+\theta}\,, \tag{19}$$

in which $\tilde{\boldsymbol{F}}^{n+\theta} = \theta\tilde{\boldsymbol{F}}^{n+1} + (1-\theta)\tilde{\boldsymbol{F}}^n$. The velocity field $\boldsymbol{u}^*$ does not only has to be projected on the space of divergence-free vector fields but also on those fields satisfying (17c). For that reason (19) is subtracted from (18a) and all terms involving $\tilde{\boldsymbol{S}}$ are neglected just as in the standard pressure-correction method. This yields:

$$\boldsymbol{M}\frac{\boldsymbol{u}^{n+1}-\boldsymbol{u}^*}{\Delta t} + \theta\boldsymbol{G}^T(\boldsymbol{p}^{n+1}-\boldsymbol{p}^n) + \theta\bar{\boldsymbol{G}}^T(c^{n+1}-c^n) = \boldsymbol{0} \tag{20}$$

If we pre-multiply equation (20) by $\boldsymbol{D}\boldsymbol{M}^{-1}$ respectively $\boldsymbol{R}\boldsymbol{M}^{-1}$ and apply equations (18b) and (18c) we get:

$$-\frac{\boldsymbol{D}\boldsymbol{u}^*}{\Delta t} + \theta\boldsymbol{D}\boldsymbol{M}^{-1}\boldsymbol{G}^T(\boldsymbol{p}^{n+1}-\boldsymbol{p}^n) + \theta\boldsymbol{D}\boldsymbol{M}^{-1}\bar{\boldsymbol{G}}^T(c^{n+1}-c^n) \;=\; 0, \tag{21}$$

$$\frac{Q-\boldsymbol{R}\boldsymbol{u}^*}{\Delta t} + \theta\boldsymbol{R}\boldsymbol{M}^{-1}\boldsymbol{G}^T(\boldsymbol{p}^{n+1}-\boldsymbol{p}^n) + \theta\boldsymbol{R}\boldsymbol{M}^{-1}\bar{\boldsymbol{G}}^T(c^{n+1}-c^n) \;=\; 0. \tag{22}$$

Since $\theta \boldsymbol{R}\boldsymbol{M}^{-1}\bar{\boldsymbol{G}}^T$ is a number $c^{n+1} - c^n$ may be eliminated from (22) in order to get

$$c^{n+1} - c^n = \frac{-1}{\theta \boldsymbol{R}\boldsymbol{M}^{-1}\bar{\boldsymbol{G}}^T}\{\theta \boldsymbol{R}\boldsymbol{M}^{-1}\boldsymbol{G}^T(\boldsymbol{p}^{n+1} - \boldsymbol{p}^n) + \frac{Q - \boldsymbol{R}\boldsymbol{u}^*}{\Delta t}\}, \tag{23a}$$

$$\begin{aligned} \theta \boldsymbol{D}\boldsymbol{M}^{-1}(\boldsymbol{G}^T \; - \; & \frac{\bar{\boldsymbol{G}}^T \boldsymbol{R}\boldsymbol{M}^{-1}\boldsymbol{G}^T}{\boldsymbol{R}\boldsymbol{M}^{-1}\bar{\boldsymbol{G}}^T})(\boldsymbol{p}^{n+1} - \boldsymbol{p}^n) = \frac{\boldsymbol{D}\boldsymbol{u}^*}{\Delta t} \\ + \; & \frac{\boldsymbol{D}\boldsymbol{M}^{-1}\bar{\boldsymbol{G}}^T}{\boldsymbol{R}\boldsymbol{M}^{-1}\bar{\boldsymbol{G}}^T}\frac{Q - \boldsymbol{R}\boldsymbol{u}^*}{\Delta t} \; . \end{aligned} \tag{23b}$$

Equation (23b) is a modified Laplacian-type equation to compute the pressure correction. From this correction $c^{n+1} - c^n$ is computed by (23a) and finally $\boldsymbol{u}^{n+1} - \boldsymbol{u}^n$ from (20).

Since we use an iterative linear solver it is not necessary to compute the matrix $\boldsymbol{D}\boldsymbol{M}^{-1}(\boldsymbol{G}^T - \frac{\bar{\boldsymbol{G}}^T \boldsymbol{R}\boldsymbol{M}^{-1}\boldsymbol{G}^T}{\boldsymbol{R}\boldsymbol{M}^{-1}\bar{\boldsymbol{G}}^T})$ explicitly. It is sufficient to program the corresponding matrix-vector multiplication. This is an important observation since the computed matrix is a full matrix, whereas each of its submatrices are very sparse. With respect to the preconditioning we limit ourselves to an incomplete LU decomposition of the matrix DM^{-1}. The numerical experiments treated in section 5 indicate that is a rather good preconditioner.

5 A numerical example

In order to test the methods described in sections 3 and 4 we consider a flow of water across a bundle of staggered pipes as shown in Figure 1. The computational region as plotted in Figure 2 is considered, which means that the anti-symmetric periodic boundary conditions must be applied.
The diameter of the pipes is 10.85 mm, the distance between the centroids of neighbouring pipes is 45 mm both in horizontal as in vertical directions. The mean velocity V_0 (from left to right) at the inlet is 1.06 m/s, which implies that the flow rate Q is given by $Q = 0.01235\ m^3/s$. The Reynolds number Re_D is related to the diameter D of the pipes. Following Perić [5], who solved a similar problem, the flow has been computed for three Reynolds numbers: $Re_D = 15, 45$ and 140.

Figure 6 shows the finite element mesh used, including the connection elements, which were introduced because of the antisymmetric periodicity. The corresponding finite volume grid is given in Figure 7.
The finite element method has been solved by a penalty method and a direct linear solver (profile method). In this stationary code 4 ($Re_D = 15$) to 6 ($Re = 140$) Newton iterations were necessary to converge to the final solution.

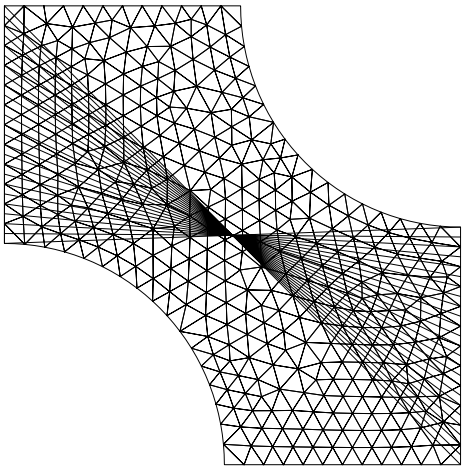

Figure 6: Finite element mesh for staggered tube problem, including connection elements

Figure 8 shows the computed streamlines for $Re_D = 140$ and Figure 9 the corresponding isobars. In order to get a clearer view of the flow and pressure distribution the computed results have been copied to a region consisting of 4 computational blocks.

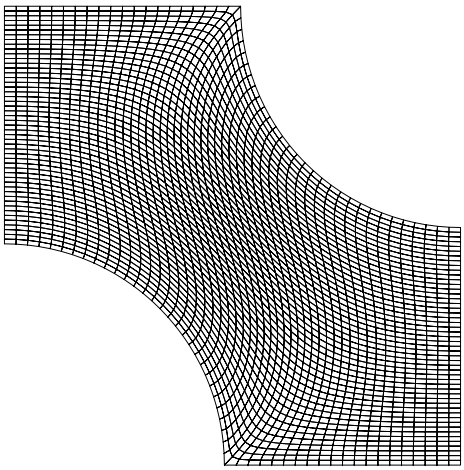

Figure 7: Finite volume grid for staggered tube problem

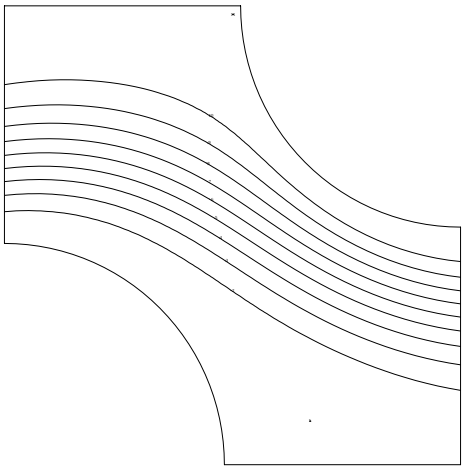

Figure 8: Streamlines in tube problem for $Re_D = 140$

Of course in the p copying of the pressure the unknown constant c is taken into account. Figures 10 and 11 show the stream lines and isobars in the compound region. The expected recirculation regions are clearly visible, just as is the case with regions of low and high pressure.

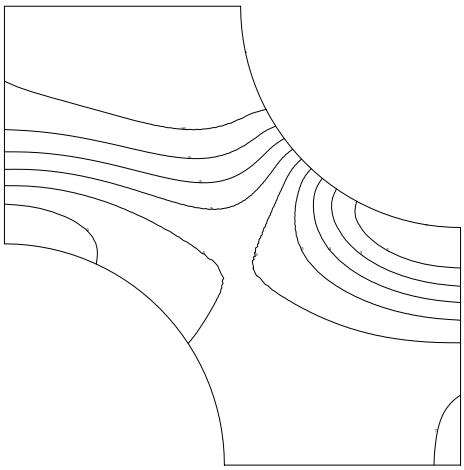

Figure 9: Isobars in tube problem for $Re_D = 140$

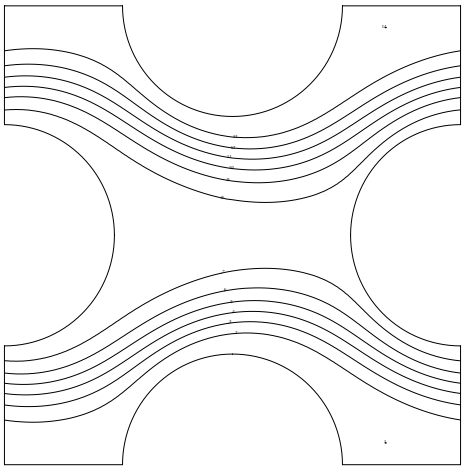

Figure 10: Streamlines in compound region consisting of 4 computational blocks

The finite volume code is instationary and based on pressure correction. The linear systems of equations were solved by a GMRESR iterative solver. The converged results were very similar to the results of the finite element code. In fact the contour plots showed no visible difference. The convergence of the constant c showed exactly the same behaviour as the convergence of the pressure to reach the stationary state. Figure 12 shows the constant c as function of time. It is clear that our algorithm gives a very good convergence.

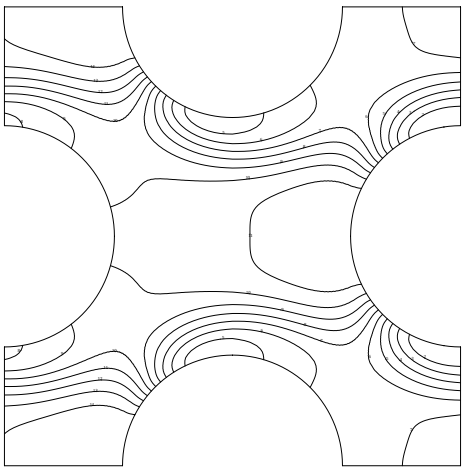

Figure 11: Isobars in compound region consisting of 4 computational blocks

To converge to steady state 75 time-steps Δt, with $\Delta t = 0.001\ s$ were necessary. The iterative solver for the momentum equations needed approximately 80 iterations for each time-step. The number of iterations for the pressure equations was about 100 per time-step, in the non-preconditioned case. Preconditioning of the pressure matrix as described in section 5 decreased the average number of iterations to 7. This shows that preconditioning based on the incomplete LU of the pressure part of (21) - (22) is an excellent preconditioner for the complete system (23b).

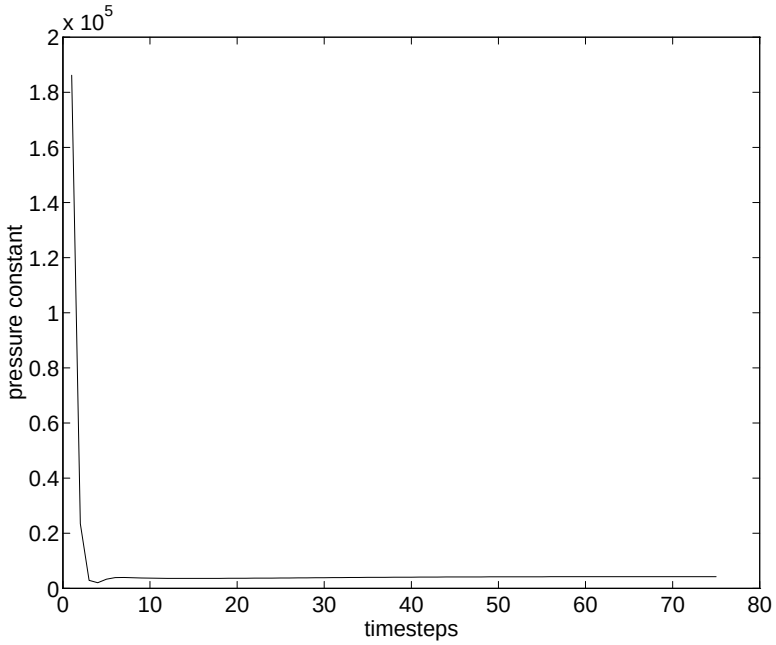

Figure 12: Convergence of the unknown constant c as function of time. $\Delta t = 0.001$

Conclusions

Two algorithms to implement periodic and antiperiodic boundary conditions in combination with a given flow rate and unknown jump in the pressure have been derived. It has been demonstrated that these algorithms converge fast and are very well suited for their purpose. Although both algorithms are completely different and must be applied in different techniques for the solution of the incompressible Navier-Stokes equations they both converge to exactly the same solution.

References

[1] C. Cuvelier, A. Segal, and A.A. van Steenhoven. *Finite element methods and Navier-Stokes equations*. Reidel Publishing Company, Dordrecht, Holland, 1986.

[2] A. Fortin. On the imposition of a flowrate by an angmented Lagrangian method. *Communications in applied Num. Methods*, 4:835–841, 1988.

[3] A.E. Mynett, P. Wesseling, A. Segal, and C.G.M. Kassels. The ISNaS incompressible Navier-Stokes solver: invariant discretization. *Applied Scientific Research*, 48:175–191, 1991.

[4] C.W. Oosterlee and P. Wesseling. A multigrid method for an invariant formulation of the incompressible Navier-Stokes equations in general co-ordinates. *Communications in Applied Numerical Methods*, 8:721–734, 1992.

[5] M. Perić. *Finite volume method for the prediction of three-dimensional fluid flow in complex ducts*. PhD thesis, Imperial College, London, 1985.

[6] A. Segal, P. Wesseling, J. Van Kan, C.W. Oosterlee, and K. Kassels. Invariant discretization of the incompressible Navier-Stokes equations in boundary fitted co-ordinates. *Int. J. Num. Meth. Fluids*, 15:411–426, 1992.

[7] D. Simonin and M. Barcouda. Measurements and predictions of turbulent flow entering a staggered tube bundle. Technical Report H-44/88.25, EDF, 1988.

[8] W.Y. Soh and J.W. Goodrich. Unsteady solution of incompressible Navier-Stokes equations. *J. of Comp. Phys.*, 79:113–134, 1988.

[9] J.J.I.M. Van Kan. A second-order accurate pressure correction method for viscous incompressible flow. *SIAM J. Sci. Stat. Comp.*, 7:870–891, 1986.

[10] C. Vuik. Solution of the discretized incompressible Navier-Stokes equations with the GMRES method. *Int. J. for Num. Meth. Fluids*, 16:507–523, 1993.

[11] P. Wesseling, A. Segal, J.J.I.M. van Kan, C.W. Oosterlee, and C.G.M. Kassels. Finite volume discretization of the incompressible Navier-Stokes equations in general coordinates on staggered grids. *Comp. Fluid Dynamics Journal*, 1:27–33, 1992.